Environmental Science and Pollution Research (2022) 29:42290–42304
https://doi.org/10.1007/s11356-021-17991-5

OCCURRENCE, IMPACT AND ELIMINATION OF CONTAMINANTS OF EMERGING CONCERN (CECS) IN SOIL, WATER AND AIR STREAMS: ADVANCES AND CHALLENGES IN IBERO-AMERICAN COUNTRIES

Environmental photochemical fate of pesticides ametryn and imidacloprid in surface water (Paranapanema River, São Paulo, Brazil)

Carolina Mendes Rocha[1] · Arlen Mabel Lastre-Acosta[1] · Marcela Prado Silva Parizi[2] · Antonio Carlos Silva Costa Teixeira[1]

Received: 24 June 2021 / Accepted: 3 December 2021 / Published online: 15 January 2022

Abstract

In addition to direct photolysis studies, in this work the second-order reaction rate constants of pesticides imidacloprid (IMD) and ametryn (AMT) with hydroxyl radicals ($HO^{\bullet}$), singlet oxygen ($^1O_2$), and triplet excited states of chromophoric dissolved organic matter ($^3CDOM^*$) were determined by kinetic competition under sunlight. IMD and AMT exhibited low photolysis quantum yields: $(1.23 \pm 0.07) \times 10^{-2}$ and $(7.99 \pm 1.61) \times 10^{-3}$ mol Einstein^{-1}, respectively. In contrast, reactions with $HO^{\bullet}$ radicals and $^3CDOM^*$ dominate their degradation, with $^1O_2$ exhibiting rates three to five orders of magnitude lower. The values of $k_{IMD,HO^{\bullet}}$ and $k_{AMT,HO^{\bullet}}$ were $(3.51 \pm 0.06) \times 10^9$ and $(4.97 \pm 0.37) \times 10^9$ L mol^{-1} s^{-1}, respectively, while different rate constants were obtained using anthraquinone-2-sulfonate (AQ2S) or 4-carboxybenzophenone (CBBP) as CDOM proxies. For IMD this difference was significant, with $k_{IMD,3AQ2S^*} = (1.02 \pm 0.08) \times 10^9$ L mol^{-1} s^{-1} and $k_{IMD,3CBBP^*} = (3.17 \pm 0.14) \times 10^8$ L mol^{-1} s^{-1}; on the contrary, the values found for AMT are close, $k_{AMT,3AQ2S^*} = (8.13 \pm 0.35) \times 10^8$ L mol^{-1} s^{-1} and $k_{AMT,3CBBP^*} = (7.75 \pm 0.80) \times 10^8$ L mol^{-1} s^{-1}. Based on these results, mathematical simulations performed with the APEX model for typical levels of water constituents (NO_3^-, NO_2^-, CO_3^{2-}, TOC, pH) indicate that the half-lives of these pesticides should vary between 24.1 and 18.8 days in the waters of the Paranapanema River (São Paulo, Brazil), which can therefore be impacted by intensive agricultural activity in the region.

Keywords Pesticides · Imidacloprid · Ametryn · Environmental persistence · Photodegradation · Mathematical simulations

Introduction

Pesticides enter the environment through extensive use in agriculture, transport of soil particles and control of aquatic weeds, reaching aquatic environments mainly through runoff, due to excess of unabsorbed rainwater (Syafrudin et al. 2021). Many effects on human health have been associated with exposure to pesticides, the most worrying being chronic poisoning, resulting in infertility, impotence, abortions, malformations, and neurotoxicity (Oliveira et al. 2014). Pesticides are also classified as endocrine disruptors, causing hormonal disturbances and interfering with the normal functioning of the endocrine system in humans and animals (Mnif et al. 2011). For this reason, monitoring of these compounds in surface water is necessary to ensure water quality and public health safety.

Among the pesticides most frequently found in ground and surface water are the herbicide ametryn (AMT) and the insecticide imidacloprid (IMD) (Montagner et al. 2019). Ametryn (AMT) (4-N-ethyl-6-methylsulfanyl-2-N-propan-2-yl-1,3,5-triazine-2,4-diamine) belongs to the chemical group of triazines, which are used extensively to control weeds, due to their ability to inhibit photosynthesis (Tarley et al. 2017). AMT is commonly found in surface and groundwater, as it is hardly adsorbed onto the soil. As this compound is characterized by being moderately toxic to

Responsible Editor: Ester Heath

✉ Carolina Mendes Rocha
carolinamr@usp.br

[1] Research Group in Advanced Oxidation Processes (AdOx), Chemical Systems Engineering Center, Department of Chemical Engineering, Escola Politécnica, University of São Paulo, Av. Prof. Luciano Gualberto, tr. 3, 380, São Paulo, SP, Brazil

[2] Energy Engineering Department, São Paulo State University (UNESP), Av. dos Barrageiros, 1881, Rosana, SP, Brazil

fish, highly toxic to crustaceans, and moderately to highly toxic to mollusks (Jacomini et al. 2009), its presence in aquatic environments becomes alarming. In addition, AMT has the potential to accumulate in sediments and aquatic biota (Jacomini et al. 2011). In turn, imidacloprid (IMD) ((NE)-N-[1-[(6-chloropyridin-3-yl)methyl]imidazolidin-2-ylidene]nitramide) is a neonicotinoid insecticide, which acts on the central nervous system of insects, where they bind to nicotinic acetylcholine receptors (nAChRs), inducing neuromuscular paralysis and eventually death (El-Akaad et al. 2020). Due to its low selectivity, this pesticide is also capable of causing damage to pollinators such as bees, affecting their locomotion or even causing the death of these animals (Kim et al. 2017). Classified by USEPA as highly toxic to aquatic invertebrates, it also has the potential to contaminate and persist in surface waters (Starner and Goh 2012). Moreover, Guo et al. (2020a) evaluated the damage caused to human lymphoblastoid TK6 cells by prolonged exposure to IMD, at a concentration of 0.1 μg L^{-1}, concluding that the insecticide can cause genetic mutations. The presence of these pollutants in reservoirs can therefore cause difficulties in guaranteeing quality water for public supply (Neto and Sarcinelli 2009). IMD has been found in maritime regions and surface waters in countries such as Canada and the Netherlands, in the concentration range of 2–193 ng L^{-1} (Van Dijk et al. 2013; Lalonde and Garron 2020). AMT, in turn, has been detected in rivers flowing to the coast in regions located near coral reefs in Australia, at concentrations between 0.11 and 2.3 ng L^{-1} (Mitchell et al. 2005; Kennedy et al. 2012). Regarding the presence of these pesticides in surface waters in Brazil, some studies found concentrations ranging from 0.03 μg L^{-1} to 72 ng L^{-1} for AMT and 8.1 ng L^{-1} to 0.9 mg L^{-1} for IMD (Monteiro et al. 2014; Rocha et al. 2015; Machado et al. 2016).

The persistence and fate of pollutants in the environment depend on biotic and abiotic processes (hydrolysis, photolysis, volatilization, complexation, oxidation, dilution, sorption, biodegradation, and/or accumulation). In natural waters, photochemical reactions driven by solar radiation play an important role in pesticide degradation (Starling et al. 2019). Direct photolysis depends on the absorption of sunlight by contaminants, whereas in indirect photolysis, pollutants react with reactive photoinduced species (RPS), such as hydroxyl radicals ($HO^{\bullet}$), singlet oxygen ($^1O_2$), and triplet exited states of chromophoric dissolved organic matter (^{3}CDOM*). RPS are generated by the interaction of sunlight with waterborne chemical species, such as nitrate, nitrite, and humic substances (Mompelat et al. 2009; Vione et al. 2010; Vione 2020). Thus, knowing the persistence of emerging pollutants in environmental waters is necessary to assess their impacts and propose actions that ensure the preservation of water resources. Carena et al. (2020) studied the photodegradation of the herbicide bentazone (BNTZ) through the irradiation of solutions prepared with water samples from lakes and rice fields in the Piedmont region, in Italy. The authors concluded that at pH 7 direct photolysis was the main BNTZ degradation mechanism. Silva et al. (2015) evaluated the photochemical behavior of the herbicide amicarbazone in aqueous systems, whose main degradation pathway depends on reactions with hydroxyl radicals. Regarding insecticides, Dell'Arciprete et al. (2010) studied the kinetics and reaction mechanisms of thiacloprid and acetamiprid with singlet oxygen and the triplet state of Rose bengal. According to the authors, the half-lives of the target contaminants through reactions with $^1O_2$ usually varied between 7 h and 21 days. In turn, Derbalah et al. (2020) investigated the influence of $^1O_2$ and $HO^{\bullet}$ on the degradation of two carbamate insecticides, methomyl and carbaryl, concluding that indirect photolysis in the presence of $HO^{\bullet}$ resulted in 60% and 62% degradation, respectively, while reactions with $^1O_2$ resulted in 26% and 30% degradation, respectively.

Considering that there are few works in the scientific literature on the photochemical persistence of pesticides in natural waters, the aim of the present study is to investigate the photochemical fate of ametryn (AMT) and imidacloprid (IMD) in aqueous media as a result of exposure to sunlight and reactions with $HO^{\bullet}$, $^1O_2$ and ^{3}CDOM*. The photochemical degradation of these pesticides was then simulated taking into account the different conditions of pH, depth of the water layer, and concentrations of dissolved organic matter and inorganic species found in a Brazilian water body (Paranapanema River), located in a region of intensive sugarcane cultivation.

Materials and methods

Reagents

Ametryn (AMT, $C_9H_{17}N_5S$) and imidacloprid (IMD, $C_9H_{10}ClN_5O_2$) were purchased from Sigma-Aldrich and employed as model pesticides of emerging concern. Hydrogen peroxide, furfuryl alcohol (FFA), parachlorobenzoic acid (*p*CBA), anthraquinone-2-sulfonate (AQ2S), 4-carboxybenzophenone (CBBP), and 2,4,6-trimethylphenol (TMP) were all of reagent grade purity and purchased from Sigma-Aldrich; methylene blue was acquired from Synth. All the solutions were prepared using deionized water (18.2 MΩ cm) from a Milli-Q® Direct-Q system (Millipore).

Photodegradation experiments under simulate solar light

Photodegradation experiments were performed using a solar simulator Peccell PEC-L01, equipped with a Xenon lamp, providing 43 W m^{-2} in the wavelength range 290–800 nm (Fig. 1). The samples were placed in 2-mL Pyrex vials with no headspace and exposed to light and kept in a water bath maintained at 24.5 °C. The radiation source was positioned over the vials at a distance of 15 cm from the liquid surface; the irradiated path length inside the vials was 10 mm. The experiments were performed in duplicates. The initial concentration of both pesticides was fixed at 10 mg L^{-1}, which is suitable for kinetic competition experiments and allows quantification by HPLC without the use of pre-concentration steps. Likewise, other studies on the photochemical fate of pollutants were conducted in the same mg L^{-1} range (Gornik et al. 2021; Carena et al. 2020; Vione et al. 2011).

Kinetic study

In order to determine the second-order rate constants of the reactions between the pesticides and RPS ($HO^{\bullet}$, $^1O_2$, and $^3CDOM^*$), the kinetic competition method described by Shemer et al. (2006) was used. All the competition kinetic experiments were performed in duplicates. The method consists of irradiating a mixture containing a compound generating the RPS, the pesticide, and a reference compound, whose reactivity with each RPS under conditions identical to the experimental system is known. Under these conditions, the second-order reaction rate constant between the RPS species of interest and the pesticide is calculated by Eq. 1:

$$k_{\mathrm{P,RPS}} = \frac{(k\mathrm{p}(obs) - k\mathrm{p}(dir.\mathrm{photo}))}{(k\mathrm{ref}(obs) - k\mathrm{ref}(dir.\mathrm{photo}))} \times k_{\mathrm{ref,RPS}} \quad (1)$$

where $k_{\mathrm{P,RPS}}$ is the second-order rate constant of the reaction between the pesticide and each RPS ($HO^{\bullet}$, $^1O_2$, and $^3CDOM^*$); $k_{\mathrm{P}(obs)}$ and $k_{\mathrm{ref}(obs)}$ correspond to the experimental pseudo-first-order degradation rate constant of the pesticide and reference compound, respectively; and $k_{\mathrm{ref,RPS}}$ is the second-order kinetic rate constant of the reaction between the reference compound and each RPS, the value of which is known from the literature. The terms $k_{\mathrm{P}(dir.\ photo)}$ and $k_{\mathrm{ref}(dir.\ photo)}$ correspond to the pseudo-first-order photolysis rate constants of the pesticide and reference compound, respectively.

In this study, *p*CBA, FFA, and TMP were used as the reference compounds in the kinetic competition experiments for $HO^{\bullet}$, $^1O_2$, and $^3CDOM^*$, respectively; in all cases, the pesticide:reference compound molar ratio was fixed at 1:1 ($[IMD]_0 = 39.1$ µmol L^{-1} and $[AMT]_0 = 43.9$ µmol L^{-1}). Additionally, H_2O_2 (50 mmol L^{-1}) and methylene blue (31.3 µmol L^{-1}) were used as the sources of $HO^{\bullet}$ and $^1O_2$, respectively. In nature CDOM is a mixture of over a thousand compounds; thus, $^3CDOM^*$ is not yet fully understood, nor is its reactivity with pollutants, making prediction of waterborne pollutants' reactivity with this species an important issue. As an alternative, different model compounds (proxies) for CDOM have been proposed. In this work, two different proxies are compared, anthraquinone-2-sulfonate (AQ2S) (30.5 µmol L^{-1}), which has been largely used, although recently its reactivity has been considered higher than expected for $^3CDOM^*$; and 4-carboxybenzophenone (CBBP) (44.2 µmol L^{-1}), whose reactivity has been found to be closer to that of real CDOM in water bodies (Carena et al.

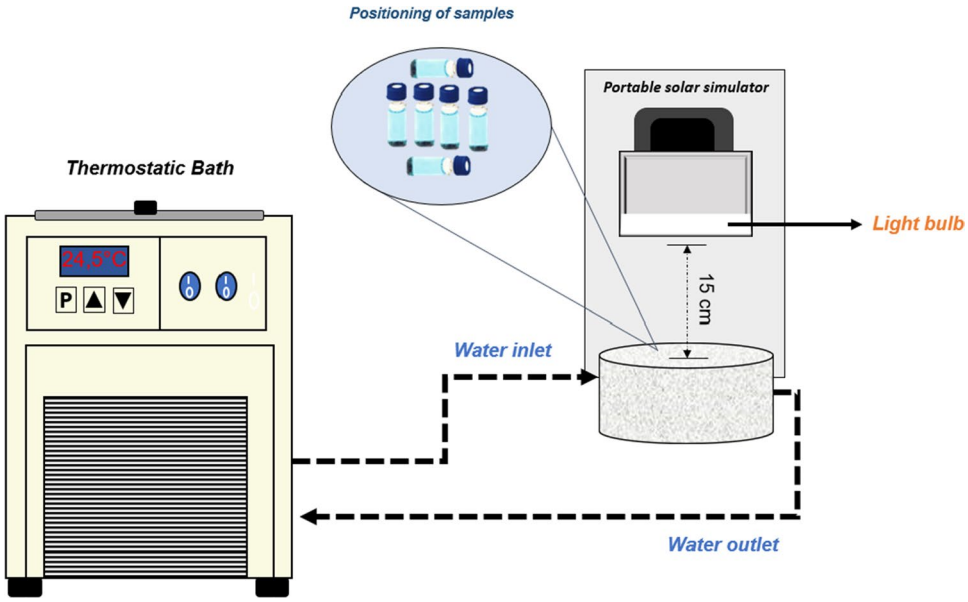

Fig. 1 Simplified scheme of the experimental equipment used in the photodegradation experiments under simulated sunlight

2019). The concentrations of H_2O_2, methylene blue, and AQ2S or CBBP were optimized in previous studies (Silva et al. 2015; Lastre-Acosta et al. 2019), in order to generate the respective RPS in excess for competition between the pesticides and reference compounds.

Water sampling

In this work, the Paranapanema River was chosen due to the fact that the region where it is located not only concentrates 80% of the sugarcane fields in the whole country, but is also a hub of agro-industries (Romangnoli and Manzione 2018). The high productivity of the sugar and alcohol sector also involves an increase in the use of pesticides, which can result in increased contamination of river waters. The Paranapanema River is located in the western region of the State of São Paulo (Brazil), and its length is approximately 929 km (Abreu et al. 2020). The samples were collected at three different points on the river (Fig. 2), whose geographical coordinates are listed in Table 1.

The following parameters were monitored: pH, temperature, and the concentrations of nitrate, nitrite, carbonate, and total organic carbon. The determination of nitrite and nitrate concentrations was performed according to the methods described in the NBR 12,619 (ABNT 1992a) and 12,620 standards (ABNT 1992b), respectively. In turn, carbonate concentrations were determined using the titration method, according to the NBR 13,736 standard (ABNT 1996). Finally, the total organic carbon (TOC) was measured using a Shimadzu TOC-L equipment.

Table 1 Geographic coordinates (south latitude/west longitude)

Point	Coordinate
1	−22.6055178/−51.906065
2	−22.555778/−52.150157
3	−22.597949/−52.873729

Simulations of the environmental photochemical persistence of pesticides

The simulation of the photochemical degradation of the pesticides and the prediction of their half-life times and main photodegradation pathways were performed using the APEX model (Vione 2020). The model considers a sunny summer day, corresponding to 10 continuous hours of irradiation at 22 W m^{-2} of irradiance. With regard to pollutants' concentrations, the model uses a default value $[P]_0 = 10^{-8}$ mol L^{-1} (Vione 2020), which can be considered environmentally significant for the pesticides studied in our work (Machado et al. 2016; Rocha et al. 2015; Monteiro et al. 2014; Britto et al. 2012). The seasonal characteristics of the Paranapanema River, as monitored monthly, together with the experimental data obtained (absorption spectra, direct photolysis quantum yields, and second-order reaction rate constants with $HO^{\bullet}$, $^1O_2$ and ^{3}CDOM*) were considered in the simulations. The values of $k_{IMD,CO3^{\bullet-}} = 4 \times 10^6$ L mol^{-1} s^{-1} (Dell'Arciprete et al. 2012) and $k_{AMT,CO3^{\bullet-}} = 7.4 \times 10^6$ L mol^{-1} s^{-1} (Canonica et al. 2005) were found in the literature. In addition, the depth of the water body was fixed at the average value of the river (2.5 m).

Fig. 2 Water sampling points in the Paranapanema River (Source: Google Earth, 2021, https://earth.google.com/web).

Analytical methods

A Shimadzu ultra-fast liquid chromatograph (UFLC, LC 20AD), equipped with a UV detector (SPD 20A) and a C18 column (SGE Wakosil®, 250 mm × 4.6 mm; 5 µm) was used to follow the concentration–time profiles of *p*CBA, FFA, and TMP. The following methods were used: *p*CBA (234 nm, 50% aqueous acetic acid 1% (v/v) + 50% methanol, isocratic); FFA (219 nm, 70% aqueous acetic acid 1% (v/v) + 30% methanol, isocratic); and TMP (220 nm, 50% aqueous acetic acid 1% (v/v) + 50% acetonitrile, isocratic). For monitoring the pesticide concentrations, a C18 column (Phenomenex Luna, 250 mm × 4.6 mm; 5 µm) and the following gradient elution method were used: Milli-Q® water (A) + methanol (B), with 50% B (0–3 min); increase to 80% B (3–12 min); 80% B (12–14 min); decrease from 80 to 50% B (14–18 min); AMT and IMD were determined at 227 and 270 nm, respectively. In all cases, the temperature, injected volume, and mobile phase flow rate were 40 °C, 100 µL, and 1 mL min^{-1}, respectively. The calibration curves were obtained from external standards prepared with known concentrations of the compounds analyzed; injections were performed in triplicates. The curves showed excellent linearity, with very low average relative errors for peak areas (< 1%), and R^2 values of 0.9984 (AMT), 0.9999 (IMD), 0.9999 (*p*CBA), 0.9994 (FFA), and 0.9998 (TMP). The limits of detection (LOD) and quantification (LOQ) were 7.8 µg L^{-1} and 23.7 µg L^{-1} for IMD, respectively, and 29.2 µg L^{-1} and 88.6 µg L^{-1} for AMT, respectively; for the reference compounds (*p*CBA, FFA and TMP), the LOD values were 2.5, 21.1, and 11.3 µg L^{-1}, respectively, while the LOQ values were 7.6, 63.9, and 34.1 µg L^{-1}, respectively. Detailed information on the calibration curves is presented in Table S1.

Results and discussion

Direct photolysis

Figure S1 shows the UV–Vis absorption spectra of IMD and AMT in aqueous solution, superimposed on the emission spectrum of the solar simulator used in the experiments. The molar absorption constants of IMD and AMT decrease above 290 nm, with $\varepsilon < 6 \times 10^3$ L mol^{-1} cm^{-1} (IMD) and $\varepsilon < 1.4 \times 10^2$ L mol^{-1} cm^{-1} (AMT), approaching zero with the wavelength going farther in the UVA and visible range. Accordingly, the time concentration profiles of IMD and AMT for direct photolysis under simulated sunlight at pH 7 (Fig. 3) show that the pesticides decayed with pseudo-first-order specific photolysis rates of $(2.06 \pm 0.13) \times 10^{-5}$ s^{-1} and $(2.17 \pm 0.43) \times 10^{-6}$ s^{-1}, respectively. The kinetic constant found for the photolysis of aqueous IMD is similar to the few values reported in the literature close to the visible range ($\lambda \geq 290$ nm), e.g., 1.6×10^{-4} s^{-1} (Moza et al. 1998), or under sunlight, i.e., 3.6×10^{-6}-3.4×10^{-5} s^{-1} (Lu et al. 2015) and 8.3×10^{-5} s^{-1} (Kurwadkar et al. 2016). According to Redlich et al. (2007), the photo-induced reaction of imidacloprid results from a triplet-controlled intermediate state, giving a series of transformation products, among which 1-[(6-chloro-3-pyridinyl)methyl]-2-imidazolidinimine is considered more toxic to warm-blooded animals than IMD. In turn, Dell'Arciprete et al. (2009) propose that the main photolysis route would involve photoreduction of the nitro-group of IMD giving the nitroso derivative, 1-[(6-chloro-3-pyridinyl)-methyl]-N-nitroso-2-imidazolidinimine, followed by internal reorganization of its nitroso-imidazolidinimine moiety to an iminodiazohydroxide and loss of N_2, yielding 1-(6-chloro-3-pyridylmethyl)imidazolidin-2-one; according to the authors, both transformation products have been observed during UVC and visible light photolysis of IMD. In the case of AMT, for which information on its direct photolysis is scarce, the magnitude of the rate constant we

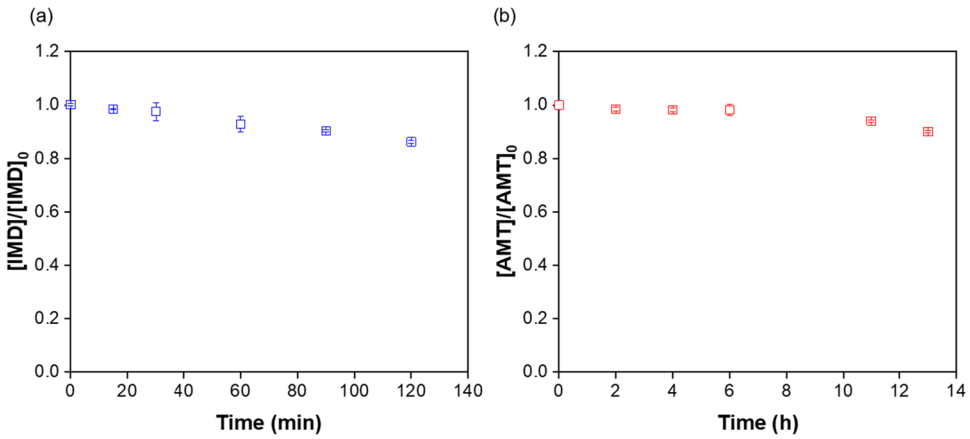

Fig. 3 Direct photolysis of IMD (**a**) and AMT (**b**) under simulated solar radiation in Milli-Q® water ($[IMD]_0 = (10.20 \pm 0.10)$ mg L^{-1}; $[AMT]_0 = (10.40 \pm 0.04)$ mg L^{-1}; at pH 7. Experiments run in duplicate

found (10^{-6} s^{-1}) is within what has been reported for herbicides, i.e., 10^{-6}–10^{-7} s^{-1} (Konstantinou et al. 2001; Lam et al. 2003; Mathon et al. 2019).

The specific photolysis rates, together with the molar absorption coefficients, were used in the present work to calculate the corresponding photolysis quantum yields in the wavelength range 290–800 nm, following the approach of Schwarzenbach et al. (2003), giving $\Phi_{IMD} = (1.23 \pm 0.07) \times 10^{-2}$ mol Einstein^{-1} and $\Phi_{AMT} = (7.99 \pm 1.61) \times 10^{-3}$ mol Einstein^{-1} (see Supplementary Materials for details on the calculation procedure). The quantum yield of IMD photolysis in sunlight that we found is in good agreement with the value reported by Todey et al. (2018), 1.05×10^{-2} mol Einstein^{-1}. Furthermore, Φ_{AMT} is similar to that of atrazine (ATZ), another triazine pesticide, under natural sunlight, i.e., 4.37×10^{-3} mol Einstein^{-1} (Wu et al. 2021) which, according to the authors, is wavelength-dependent, tending to be higher in the UVB/UVA range. The low values of Φ_{IMD} and Φ_{AMT} suggest the slow pesticide degradation in the absence of reactive photo-induced species. In addition, the results show that the degradation was significantly faster for IMD compared to AMT, which is also related to the lower values of ε for AMT in the range 290–350 nm (Figure S1). Other compounds whose quantum yields have an order of magnitude (10^{-3}–10^{-2} mol Einstein^{-1}) similar to those found for IMD and AMT, such as the pesticide diuron, also show slow degradation while irradiated under visible light (simulated or natural) in aqueous solution (Wang et al. 2020).

Second-order rate constants of the reactions between pesticides and reactive photo-induced species

Direct photolysis can only be considered efficient when the photolysis quantum yield of the pollutants is significantly high and if there is an overlap of the absorption spectrum of the pollutant with the emission spectrum of the radiant source. According to the discussion in the previous section, these requirements were not met for IMD and AMT, which is in agreement with the literature. In fact, it is known that indirect photolysis generally plays a more relevant role in the degradation of pollutants in sunlit waters (Lester et al. 2013; Zhang et al. 2020). In this case, the photodegradation of contaminants occurs by reactions with reactive photo-induced species (RPS) ($HO^{\bullet}$, $^1O_2$, and ^{3}CDOM*), which result from the absorption of light by chemical species present in water bodies, both organic and inorganic. $HO^{\bullet}$ radicals, whose concentrations in surface water are between 10^{-17} and 10^{-15} mol L^{-1} (Dell'Arciprete et al. 2009), are mainly formed by the photolysis of NO_2^- and NO_3^- (Eqs. 2–5), with quantum yields of 2.5×10^{-3}-7×10^{-3} mol Einstein^{-1} (292–430 nm) and 9.2×10^{-3}-1.7×10^{-2} mol Einstein^{-1} (290 nm), respectively (Helz et al. 2000). On the other hand, the exact mechanism of $HO^{\bullet}$ formation from chromophoric dissolved organic matter (CDOM) is not yet fully understood; however, it is known that it may involve the oxidation of water by triplet excited states of CDOM, following light absorption (Eqs. 6 and 7) (Vione et al. 2010):

$$NO_3^- + h\nu \rightarrow NO_2^- + {}^1\!/_2\, O_2 \quad (2)$$

$$NO_2^- + h\nu \rightarrow NO_2^{-*} \rightarrow NO^{\bullet} + O^{\bullet -} \quad (3)$$

$$NO_3^- + h\nu \rightarrow NO_3^{-*} \rightarrow NO_2^{\bullet} + O^{\bullet -} \quad (4)$$

$$O^{\bullet -} + H_2O \rightarrow HO^{\bullet} + HO^- \quad (5)$$

$$CDOM + h\nu \rightarrow {}^3CDOM^* \quad (6)$$

$$^3CDOM^* + H_2O \rightarrow CDOM^* - H^{\bullet} + HO^{\bullet} \quad (7)$$

In turn, singlet oxygen ($^1O_2$) is formed by energy transfer between triplet excited states of organic matter and dissolved oxygen (O_2) (Eq. 8). Since $^1O_2$ is quenched by solvent molecules (Eq. 9), its steady-state concentration near the surface of water bodies is proportional to DOM concentration, with values around 10^{-14} to 10^{-13} mol L^{-1} (Schwarzenbach et al. 2003). ^{3}CDOM* can also react directly with waterborne contaminants through electron transfer, its steady-state concentrations (10^{-14} to 10^{-12} mol L^{-1}, Mcneill and Canonica 2016) depending on the organic matter content of the aqueous matrix, which is a balance between the rates of formation and consumption by natural processes.

$$^3CDOM^* + O_2 \rightarrow CDOM + {}^1O_2 \quad (8)$$

$$^1O_2 + H_2O \rightarrow O_2 + H_2O \quad (9)$$

All transient RPS are also consumed by natural water constituents (HCO_3^-/CO_3^{2-}, NO_2^-, DOM), according to Eqs. 10–14 (Vione 2020), resulting in secondary radical species (e.g., $CO_3^{\bullet -}$, $NO_2^{\bullet}$) which can also react with contaminants molecules.

$$HO^{\bullet} + HCO_3^- \rightarrow H_2O + CO_3^{\bullet -} \quad (10)$$

$$HO^{\bullet} + CO_3^{2-} \rightarrow HO^- + CO_3^{\bullet -} \quad (11)$$

$$HO^{\bullet} + NO_2^- \rightarrow HO^- + NO_2^{\bullet} \quad (12)$$

$$HO^{\bullet} + DOM \rightarrow \text{products} \quad (13)$$

$$^{3}CDOM^{*} + CO_3^{2-} \rightarrow CDOM^{\bullet-} + CO_3^{\bullet-} \quad (14)$$

Table 2 presents the second-order kinetic rate constants of pesticide (P) reactions with the primary RPS ($HO^{\bullet}$, $^{1}O_2$, and ^{3}CDOM*), at pH 7 and $[P]_0 = 10$ mg L^{-1}, determined by competition kinetic experiments (see Supplementary Materials for the full set of results, Figures S2–S17). The magnitude of $k_{IMD,HO^{\bullet}} = (3.51 \pm 0.06) \times 10^9$ L mol^{-1} s^{-1} is consistent with previous values reported in the literature, lying in the range 10^9–10^{10} L mol^{-1} s^{-1} (Zaror et al. 2010; Dell'Arciprete et al. 2009). On the contrary, $k_{IMD,1O2} = (2.86 \pm 0.65) \times 10^5$ L mol^{-1} s^{-1} is lower than that reported by Dell'Arciprete et al. (2010), $(5.5 \pm 0.5) \times 10^6$ L mol^{-1} s^{-1}. In turn, AMT belongs to the same chemical group as atrazine (ATZ), whose rate constants have been widely discussed. The values of the reaction rate constants between ATZ and $HO^{\bullet}$ of 3×10^9 L mol^{-1} s^{-1} (Acero et al. 2000) and 2.7×10^9 L mol^{-1} s^{-1} (Marchetti et al. 2013) are similar to the value found for AMT, $k_{IMD,HO^{\bullet}} = (4.97 \pm 0.37) \times 10^9$ L mol^{-1} s^{-1}. Likewise, Marchetti et al. (2013) found $k_{ATZ,1O2} = 4 \times 10^4$ L mol^{-1} s^{-1} using Rose bengal as the source of $^{1}O_2$ which is similar to that we found for AMT using methylene blue, $k_{IMD,1O2} = (3.43 \pm 0.58) \times 10^4$ L mol^{-1} s^{-1}. Oppositely, the values of $k_{AMT,3CBBP*}$ and $k_{AMT,3AQ2S*}$ found by the kinetic competition method, in our study, are slightly smaller than the value $k_{ATZ,3CDOM*} = (1.2 \pm 0.2) \times 10^9$ L mol^{-1} s^{-1} found by Zeng and Arnold (2013) for ATZ photodegradation under natural sunlight.

The results suggest that the attack of both pesticide molecules by hydroxyl radicals and ^{3}CDOM* is expected to be the dominant mechanism in their solar-driven photodegradation, with singlet oxygen playing a minor role. In fact, the competition kinetic experiments showed 89% decrease in FFA concentration and only 7% in IMD at the end of 60 min (Figures S4 and S5); as for the experiments with AMT, there was a decay of 98% of FFA and 6% of AMT, after the same time (Figures S12 and S13). Oppositely, Zhang et al. (2020) observed that $^{1}O_2$ originating from DOM derived from pig manure biochar pyrolyzed at 500 °C played an important role in the phototransformation of IMD under UV radiation, with the loss of the nitro group and oxidation in the imidazolidine ring as the main photodegradation pathways. Dell'Arciprete et al. (2010) propose the occurrence of a charge-transfer reaction between IMD and singlet oxygen, giving superoxide radical anions ($O_2^{\bullet-}$) and the radical cation of IMD, which undergoes elimination of H^+ leading to a α-aminoalkyl radical in the methylene bridge, which subsequently reacts with dissolved oxygen and water to form 6-chloronicotinic acid. Accordingly, this reaction pathway can also be initiated after the reaction with triplet excited states of DOM (Dell'Arciprete et al. 2010). Furthermore, Kan et al. (2020) suggest that the C1 position of IMD can be attacked by $HO^{\bullet}$, resulting in the cleavage of C – N bond and forming (6-chloropyridin-3-yl) methanol, which generates 6-chloronicotinic acid through further oxidation. Additionally, Dell'Arciprete et al. (2009) argue that oxidation of IMD molecules by $HO^{\bullet}$ attack at the methylene group of the heterocycle can occur; likewise, both the methylene group bridging the heterocycles and the methylene group of the heterocycle of the photolysis product 1-(6-chloro-3-pyridylmethyl)imidazolidin-2-one ("Direct pyrolysis" section) are prone to attack by $HO^{\bullet}$ radicals, giving transformation products whose further oxidation results in the formation of 6-chloronicotinic aldehyde and 6-chloronicotinic acid. All these metabolites, according to the authors, have been reported in the photodegradation and biological degradation of IMD, with its pyridine moiety remaining intact under conditions of moderate oxidation and low levels of photolysis. In contrast, limited information is available in the literature on AMT degradation by RPS. De Oliveira et al. (2019) reported the formation of hydroxylated products and lower molecular weight intermediates through the attack of $HO^{\bullet}$ radicals on the aliphatic carbon chain of the AMT molecule and/or sulfur in the R–S–CH_3 group, through UV_{254}/H_2O_2, Fenton and photo-Fenton processes.

According to Remucal (2014), information on photodegradation in the presence of chromophoric dissolved organic matter (CDOM) for insecticides and herbicides is limited. The order of magnitude of the rate constants for IMD and AMT in Table 2 is in line with the information that ^{3}CDOM* would play an important role in the degradation of pollutants in sunlit waters (Lastre-Acosta et al. 2019). Two values were obtained for each pesticide, one for each proxy used. According to Avetta et al. (2016), CBBP has been used as a proxy of CDOM, since its triplet excited state is less reactive when compared to ^{3}AQ2S*. This fact explains why IMD degradation was slower in the presence of CBBP (see Figures S6 and S8). Accordingly, distinct second-order

Table 2 Second-order kinetic rate constants for pesticides reactions with reactive photo-induced species under simulated sunlight in Milli-Q® water at pH 7

Pesticide	$k_{P,HO^{\bullet}}$ (L mol^{-1} s^{-1})	$k_{P,1O2}$ (L mol^{-1} s^{-1})	$k_{P,3CBBP*}$ (L mol^{-1} s^{-1})	$k_{P,3AQ2S*}$ (L mol^{-1} s^{-1})
IMD	$(3.51 \pm 0.06) \times 10^9$	$(2.86 \pm 0.65) \times 10^5$	$(3.17 \pm 0.13) \times 10^8$	$(1.02 \pm 0.08) \times 10^9$
AMT	$(4.97 \pm 0.37) \times 10^9$	$(3.43 \pm 0.58) \times 10^4$	$(7.75 \pm 0.80) \times 10^8$	$(8.13 \pm 0.68) \times 10^8$

Table 3 Results of the parameters selected for monitoring the Paranapanema River water, together with the predicted mean half-life times

Sampling point	$[CO_3^{2-}]$ (mg L^{-1})	$[NO_2^-]$ (mg L^{-1})	$[NO_3^-]$ (mg L^{-1})	TOC (mg L^{-1})	pH	$t_{1/2}$ (IMD) (days)	$t_{1/2}$ (AMT) (days)
Dec/2019							
1	27.0 ± 1.0	(0.011 ± 0.001)	1.12 ± 0.53	12.1 ± 1.0	7.40 ± 0.01	25.97	20.00
2	37.0 ± 1.0	(0.013 ± 0.001)	2.24 ± 0.32	11.9 ± 0.0	7.36 ± 0.01	25.97	19.96
3	38.0 ± 0.0	(0.010 ± 0.000)	1.38 ± 0.14	12.4 ± 0.6	7.36 ± 0.01	26.23	20.04
Feb/2020							
1	37.5 ± 0.5	(0.0083 ± 0.0004)	0.47 ± 0.14	12.9 ± 0.5	7.59 ± 0.04	26.83	20.12
2	24.0 ± 0.0	(0.0091 ± 0.0003)	0.98 ± 0.09	9.42 ± 0.02	7.23 ± 0.005	22.65	19.46
3	25.0 ± 1.0	(0.0096 ± 0.0001)	1.27 ± 0.42	9.51 ± 0.07	7.23 ± 0.01	22.77	19.48
May/2020							
1	33.0 ± 1.0	(0.0120 ± 0.0006)	1.13 ± 0.10	11.9 ± 1.6	7.93 ± 0.05	25.70	19.97
2	29.0 ± 1.4	(0.0120 ± 0.0001)	0.71 ± 0.03	4.7 ± 0.9	7.45 ± 0.05	14.28	16.80
3	28.0 ± 0.0	(0.0120 ± 0.0006)	1.17 ± 0.00	6.5 ± 1.3	7.44 ± 0.005	17.89	18.23
Jul/2020							
1	27.0 ± 1.0	(0.0100 ± 0.0004)	0.75 ± 0.08	5.3 ± 0.3	7.75 ± 0.05	15.68	17.42
2	40.0 ± 0.0	(0.0090 ± 0.0004)	0.65 ± 0.03	12.0 ± 0.3	7.51 ± 0.03	25.86	10.00
3	24.0 ± 1.0	(0.010 ± 0.001)	0.84 ± 0.04	4.2 ± 0.1	7.52 ± 0.02	13.11	16.21
Aug/2020							
1	28.0 ± 0.0	(0.0080 ± 0.0007)	1.45 ± 0.02	8.3 ± 0.5	7.48 ± 0.04	20.95	19.09
2	26.0 ± 0.0	(0.0130 ± 0.0001)	2.58 ± 0.06	18.9 ± 3.9	7.13 ± 0.02	31.71	20.60
3	24.0 ± 0.0	(0.009 ± 0.000)	1.36 ± 0.12	15.4 ± 0.2	7.52 ± 0.03	29.09	20.37
Sep/2020							
1	28.0 ± 0.0	(0.0130 ± 0.0003)	0.81 ± 0.20	12.0 ± 0.4	7.85 ± 0.10	25.84	19.99
2	28.0 ± 0.0	(0.0130 ± 0.0002)	1.28 ± 0.04	13.0 ± 0.4	7.32 ± 0.03	26.86	20.12
3	26.0 ± 0.0	(0.0170 ± 0.0009)	1.20 ± 0.07	4.4 ± 0.3	7.34 ± 0.01	13.68	16.50
Oct/2020							
1	31.0 ± 1.0	(0.0200 ± 0.0012)	0.57 ± 0.16	11.0 ± 3.3	7.96 ± 0.02	24.66	19.82
2	26.0 ± 0.0	(0.0150 ± 0.0001)	1.48 ± 0.31	15. 5 ± 1.9	7.71 ± 0.00	29.13	20.38
3	26.0 ± 0.0	(0.0180 ± 0.0008)	0.76 ± 0.01	6.6 ± 0.4	7.54 ± 0.005	18.19	18.34
Nov/2020							
1	30.0 ± 0.0	(0.0030 ± 0.0003)	0.49 ± 0.00	17.3 ± 0.6	8.36 ± 0.02	30.61	20.52
2	26.0 ± 0.0	(0.0030 ± 0.0003)	0.35 ± 0.12	5.4 ± 0.6	7.61 ± 0.02	15.83	17.49
3	24.0 ± 0.0	(0.0060 ± 0.0006)	0.60 ± 0.23	11.7 ± 0.1	7.56 ± 0.04	48.44	19.95

kinetic rate constants were obtained at pH 7, $k_{IMD,3AQ2S^*} = (1.02 \pm 0.08) \times 10^9$ L mol^{-1} s^{-1} and $k_{IMD,3CBBP^*} = (3.17 \pm 0.14) \times 10^8$ L mol^{-1} s^{-1}. Avetta et al. (2016) compared the rate constants for naproxen and clofibric acid, using CBBP and AQ2S. The second-order reaction rate constants with AQ2S found by the authors were an order of magnitude higher than those obtained with CBBP, which is in agreement with the results we obtained. With respect to AMT, we observed that the degradation of the herbicide also occurred more slowly in the presence of CBBP (Figure S16) compared to the experiment in which AQ2S was used (Figure S14), although the choice did not substantially impact the rate constants obtained by competition kinetics, $k_{AMT,3AQ2S^*} = (8.13 \pm 0.35) \times 10^8$ L mol^{-1} s^{-1} and $k_{AMT,3CBBP^*} = (7.75 \pm 0.80) \times 10^8$ L mol^{-1} s^{-1}. Carena et al. (2019) compared the constants obtained experimentally using CBBP with values available in the literature based on AQ2S, finding that atrazine (ATZ) had quite similar reaction rates for the two proxies ($k_{ATZ,3AQ2S^*} = 1.4 \times 10^9$ L mol s^{-1} and $k_{ATZ,3CBBP^*} = 0.7 \times 10^9$ L mol s^{-1}). From these results, it can be concluded that both CBBP and AQ2S can be used to correctly assess the reactivity of the two triazine herbicides, AMT and ATZ, with ^{3}CDOM*.

Characterization of the Paranapanema River water and simulation of photochemical environmental persistence of the pesticides

The parameters monitored (pH, concentrations of nitrate, nitrite, carbonate, and total organic carbon-TOC) are related

to the quantification of the RPS formed in the water bodies, which are essential for determining the photochemical persistence of pollutants in real matrices. The results are shown in Table 3. The mean concentration of nitrite found for the three sampling points in the monitored months was (0.01100 ± 0.00005) mg L^{-1}. As for nitrate, the mean concentrations found in all monitored points of the Paranapanema River were (1.070 ± 0.006) mg L^{-1}. Although no significant changes were observed in the concentrations of nitrite and nitrate, it can be seen that in February (summer) and November (spring) their values were slightly lower. This can be explained by the fact that the region has a rainy tropical climate with dry winters, so that in these months there is high rainfall, and lower concentrations may be associated with the dilution effect. Also, seasonality had no notable influence on pH and CO_3^{2-} concentrations. In contrast, the total organic carbon (TOC) seemed to be more influenced by seasonality and sampling point, exhibiting an average value of (10.26 ± 0.39) mg L^{-1}.

The mathematical simulations were carried out based on the measured direct photolysis quantum yields and second-order rate constants of the reactions between each pollutant and the RPS, considering the characteristics of the Paranapanema River, for an average depth of the water body of 2.5 m. In this work, the mathematical simulations were performed using $k_{IMD,3CPPB*}$ and $k_{AMT,3CPPB*}$ as conservative estimates of pollutants reactivity with ^{3}CDOM*, as previously discussed. The estimated average mean half-lives of IMD and AMT are (24.1 ± 7.6) and (18.8 ± 2.3) days, respectively (Table 3), which are within the range of values described in the literature. In fact, the USEPA reports that $t_{1/2}$ of IMD in water ranges from 0.2 to 29 days (Starner and Goh, 2012), and according to Bonmatin et al. (2015) and Guo et al. (2020b), despite the degradation of IMD when subjected to photolysis, the compound can remain in aquatic environments and in sediments, and in this case its half-life can reach 30–162 days. With regard to AMT, the half-life of the herbicide in water is around 22 and 28 days, according to USDA (2006) and Kegley et al. (2014), respectively. In addition, Konstantinou et al. (2001) evaluated the degradation of triazine herbicides (atrazine, propazine, and prometryne) under natural sunlight in different waters (river, lake, sea, groundwater, and distilled water), reporting that $t_{1/2}$ for these herbicides ranges from 26 to 73 days. Considering the ranges of values of $[NO_3^-]$, $[NO_2^-]$, $[CO_3^{2-}]$, and [TOC] used in the simulations, it can be said that the concentration of TOC (i.e., dissolved organic matter content) seems to be the parameter that most significantly impacted the values of $t_{1/2}$ obtained in our work. This can be attributed to the fact that TOC was noticeably influenced by the sampling point and season of the year, varying in the range 4.2–18.9 mg L^{-1}. Although seasonality has not been a highly relevant factor for the variation in TOC concentration, it is expected that in rainy periods the concentration of organic matter is lower due to dilution, suggesting a scenario in which pesticide half-lives may be smaller.

Also based on the characteristics of the water body, the first-order degradation rate constants corresponding to each of the main photo-induced pathways (direct photolysis and attack by ^{3}CDOM* and $HO^\bullet$) were also obtained, in all seasons, for all three monitoring points (Figs. 4 and 5). With these constants, the pesticides' half-lives for each of these routes were estimated using the APEX model and Eq. 15. Since the experimental second-order kinetic degradation rate constants found for the reactions of IMD and AMT with $^1O_2$ were three to five orders of magnitude lower compared to those obtained for $HO^\bullet$ radicals and ^{3}CDOM* (Table 2), the half-lives predicted from kinetic simulations considering only the reactions of pesticides with singlet oxygen were very large, on the order of months, and therefore are not included in these graphs.

$$t_{1/2} = \ln 2 k^{-1} \tag{15}$$

It can be inferred that the degradation of both pesticides occurs mainly by direct photolysis and reactions with ^{3}CDOM*, the latter particularly influencing the degradation of AMT. As reported by Vione et al. (2018), photodegradation mediated by ^{3}CDOM* tends to be faster for higher concentrations of organic matter in the water, in this work evaluated through the concentration of TOC. On the other hand, when the organic matter content decreases, direct photolysis then becomes the main pollutants' degradation route. Noteworthy, IMD degradation appears to be more influenced by seasonality and geographic location compared to AMT.

Additionally, the depth of the water body plays an important role in the photodegradation of pollutants, which tends to be favored in shallower environments, since the surface layer is fully illuminated while the bottom is darker, thus inhibiting the process (Vione and Scozzaro 2019; Vione et al. 2018). Therefore, simulations were performed varying the water depth to understand the influence of this parameter on the environmental fate of the pesticides in the Paranapanema River. For these simulations, the maximum concentrations of the parameters in Table 3 were defined for each of the sampling points. As can be seen in Fig. 6, the degradation of the pesticides becomes considerably slower as the depth increases, with the half-lives increasing linearly, particularly for AMT.

In addition to the depth, the average flow velocity of the river water also plays an important role in the assessment of pesticides photodegradation. This is because the velocity interferes with the pollutant's residence time in the water bodies. In periods of intense drought, the volume and water velocities of rivers decrease, making photochemical-driven processes more efficient in comparison with rainy periods, in

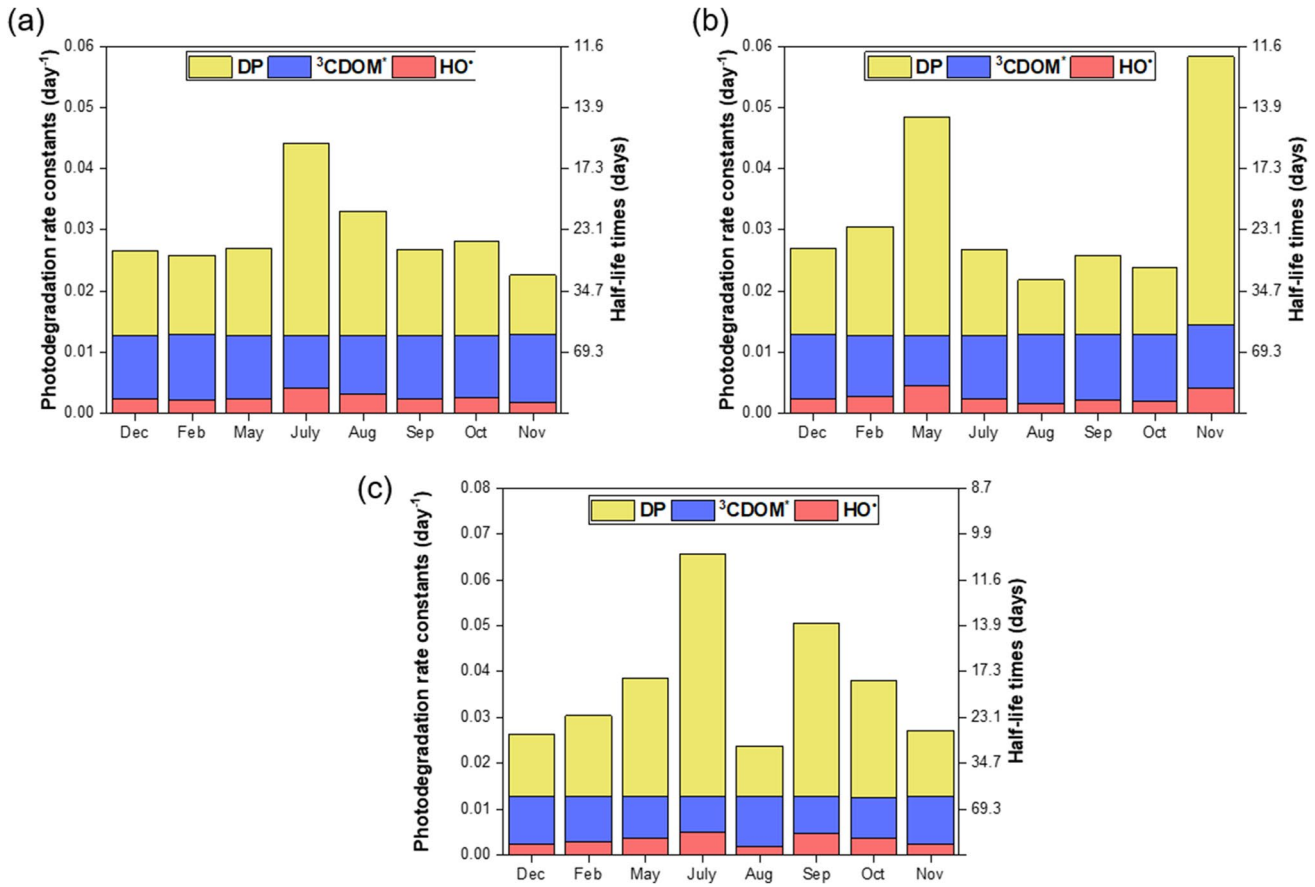

Fig. 4 Predicted rate constants of IMD photodegradation in the Paranapanema River induced by the main photochemical processes (direct photolysis-DP and attack by $^3CDOM^*$ and $HO^\bullet$). **a** Point 1, **b** Point 2, and **c** Point 3

which they are often insignificant (Carena et al. 2021; Vione and Scozzaro 2019). That is why it is necessary to measure the half-life length, which consists of the length of the illuminated path necessary to halve the concentration of the pollutant (Vione 2020). The half-life length ($l_{1/2}$) can be calculated using Eq. 16, where $\bar{v}$ corresponds to the average water flow velocity of the Paranapanema River (0.15–0.85 m s^{-1}, according to Granado et al. 2009), and $t_{1/2}$ is the predicted half-life time (Carena et al. 2021).

$$l_{1/2} = \bar{v}\, t_{1/2} \tag{16}$$

From Eq. 16 and considering half-lives of up to 40 days, it can be found that the values of $l_{1/2}$ vary in the range from 518.4 to 2937.6 km for $\bar{v} = 0.15$ and 0.85 m s^{-1}, respectively. Therefore, considering that point 1 is 27.65 km from point 2, which is 80.53 km from point 3, the half-life length required to degrade both IMD and AMT is greater than the distance between the sampling points. It is possible to infer two effects from this information. The first is that the degradation rates increase as the water flow rate decreases, resulting in shorter half-lives, favoring photodegradation. The second is that the river is not long enough to guarantee to halve the concentration of the pesticides, for which $t_{1/2}$ lies in the range 19 to 24 days.

Finally, half-life estimates were obtained using the values of $k_{P,3AQ2S*}$ and $k_{P,3CBBP*}$ to assess the impact of different model compounds (proxies) in predicting the persistence of IMD and AMT in sunlit waters. For these simulations, the maximum and minimum concentrations of the input parameters for each of the sampling points of the Paranapanema River were selected. The results are shown in Table S2. The choice of proxies for CDOM (AQ2S or CBBP) did not influence the measured values of $k_{AMT,3CDOM*}$ for AMT, both being suitable for evaluating the degradation kinetics of this herbicide by triplet excited states of chromophoric dissolved organic matter; therefore, the respective estimated half-lives do not differ significantly (Table S2). In contrast, for IMD the experimental values of $k_{IMD,3CDOM*}$ were more impacted by the choice of the CDOM model, resulting in $t_{1/2}$ values with differences of up to 10 days, reinforcing the need to properly select the proxy to avoid the photochemical persistence of emerging contaminants such as IMD being underestimated.

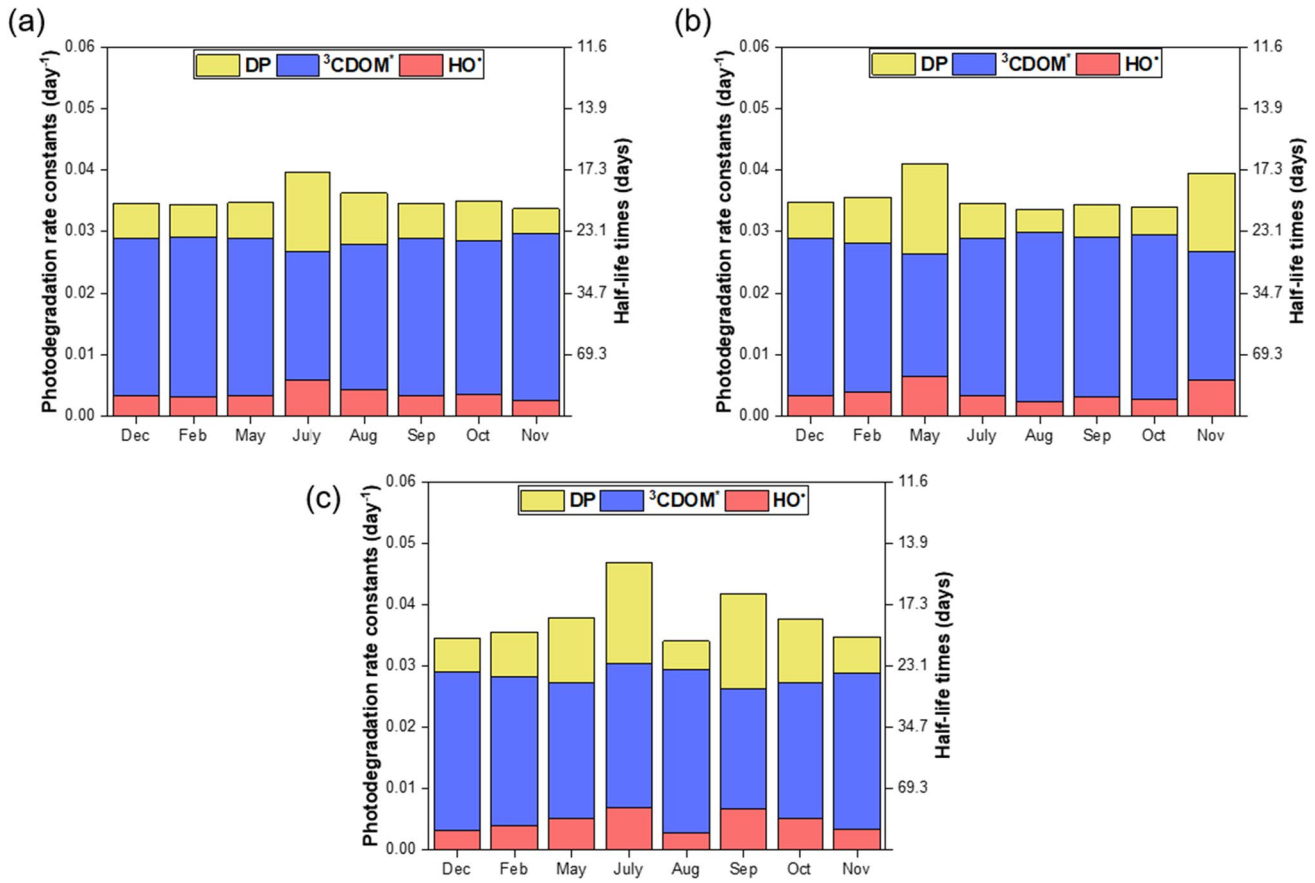

Fig. 5 Predicted rate constants of AMT photodegradation in the Paranapanema River induced by the main photochemical processes (direct photolysis-DP and attack by $^{3}CDOM^{*}$ and $HO^{\bullet}$). **a** Point 1, **b** Point 2, and **c** Point 3

Conclusions

Photo-induced reactions represent one of the main pathways of pollutant degradation in water, promoted by solar radiation and the action of reactive species, that is, by direct and indirect photolysis. In our work, we aimed to investigate the photochemical fate of two pesticides, imidacloprid (IMD) and ametryn (AMT) in sunlit water. In addition to photolysis studies, the second-order reaction rate constants of IMD and AMT with reactive photo-induced species-RPS (hydroxyl radicals, $HO^{\bullet}$; singlet oxygen, $^{1}O_2$; and triplet excited states of chromophoric dissolved organic matter, $^{3}CDOM^{*}$) were determined by the kinetic competition method at pH 7. Direct photolysis relies on the absorption of sunlight by contaminants, a process that is only efficient if the contaminant's absorption spectrum overlaps with the solar emission spectrum. This was not the case for IMD and AMT, which exhibited low direct photolysis quantum yields under simulated sunlight, $\Phi_{IMD} = (1.23 \pm 0.07) \times 10^{-2}$ mol Einstein^{-1} and $\Phi_{AMT} = (7.99 \pm 1.61) \times 10^{-3}$ mol Einstein^{-1}.

The results obtained in this work confirmed that hydroxyl radicals have an important effect on the degradation of both pesticides, with second-order kinetic rate constants at pH 7 of $k_{IMD,HO^{\bullet}} = (3.51 \pm 0.06) \times 10^{9}$ L mol^{-1} s^{-1} and $k_{AMT,HO^{\bullet}} = (4.97 \pm 0.37) \times 10^{9}$ L mol^{-1} s^{-1}. Reactions with $^{3}CDOM^{*}$ should also contribute to pesticide degradation in surface water, with second-order rate constants an order of magnitude lower. Different values of kinetic constants were obtained using anthraquinone-2-sulfonate (AQ2S) or 4-carboxybenzophenone (CBBP) as proxies to estimate the reaction kinetics between the pesticides and organic matter in the triplet state. For IMD this difference was significant, on the contrary, the values found for AMT are close. These results highlight the need to carefully consider which model compound (proxy) to use, as for some pollutants there is a risk of underestimating the real value. That said, regardless of the choice of proxy and although the values of $k_{pollutant,3CDOM^{*}}$ may vary, its determination is a valuable reference given its importance in pesticides degradation. On the other hand, unlike other RPS, $^{1}O_2$ did not significantly affect IMD and AMT degradation, exhibiting rates three to five orders of magnitude lower compared to those obtained for $HO^{\bullet}$ radicals and $^{3}CDOM^{*}$.

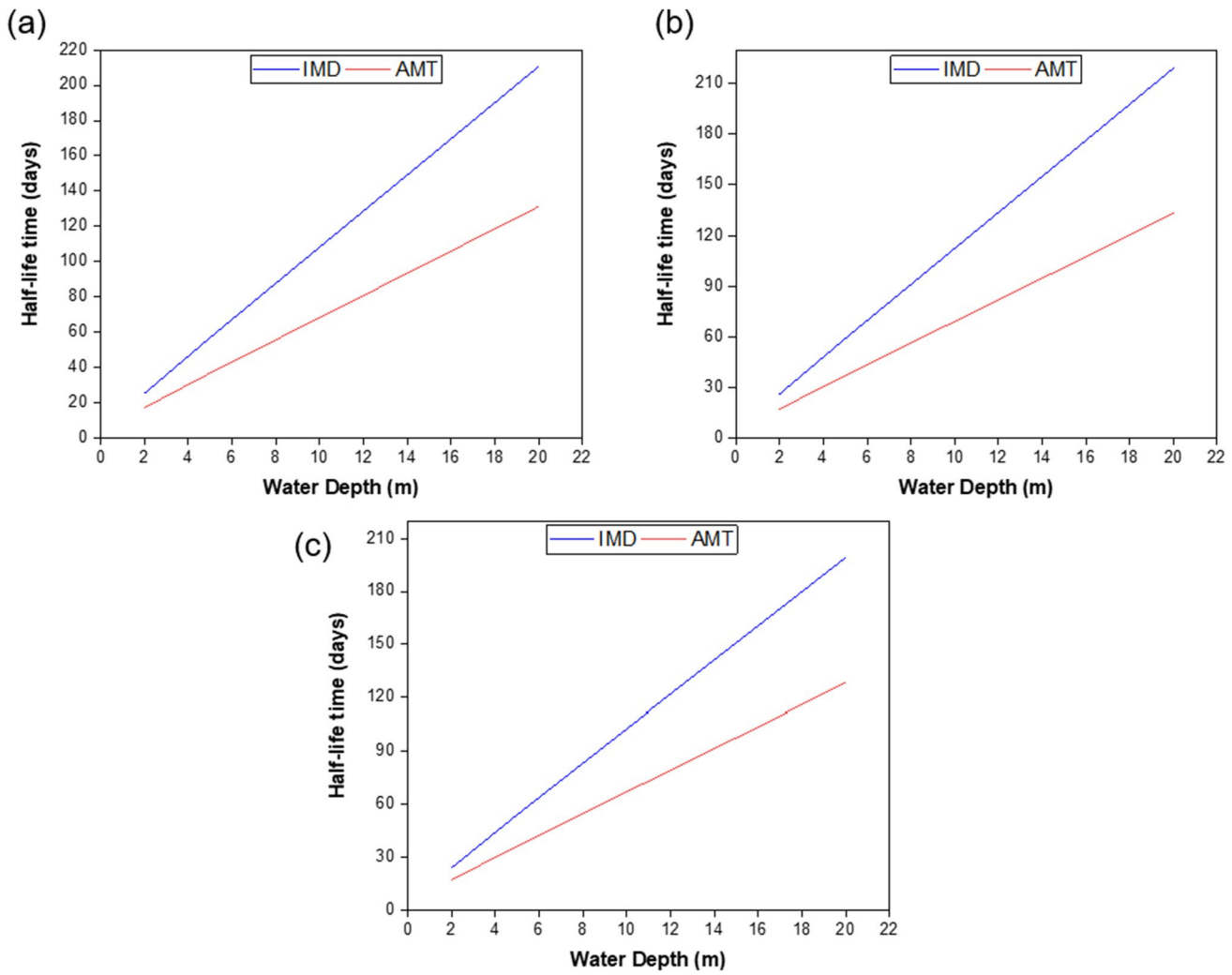

Fig. 6 Predicted half-life times of IMD and AMT as function of the water depth. **a** Point 1, **b** Point 2, and **c** Point 3

Simulations of the environmental photochemical persistence of pesticides, performed using the APEX model and taking into account the different conditions of pH, depth of the water layer, and concentrations of dissolved organic matter and inorganic species, indicated predicted half-lives of IMD and AMT of about 24.1 and 18.8 days, respectively, considering the ranges of values found for $[NO_3^-]$, $[NO_2^-]$, $[CO_3^{2-}]$, and [TOC] in the monitoring of the Paranapanema River. It was noticed that the depth of the river, the speed of water flow, and the concentration of organic matter are the factors that most influence pesticide degradation. Thus, shallower watercourses and with lower flow rates result in longer detention times, which favors the photodegradation of contaminants.

In summary, the results we present in this work constitute essential information to understand the extent of persistence of imidacloprid and ametryn in environmental waters in regions of intensive agricultural activity—mainly sugarcane cultivation—as well as to assess their impacts on ecosystems and propose actions to ensure the preservation of water resources and the quality of water for public supply, given the hazardous characteristics of these contaminants.

Supplementary Information The online version contains supplementary material available at https://doi.org/10.1007/s11356-021-17991-5.

Acknowledgements The authors are grateful to the São Paulo Research Foundation (FAPESP) (grants #2019/24158-9 and 2019/00696-1) and to the National Council for Scientific and Technological Development – Brazil (CNPq) (grant #311230/2020-2).

Author contribution CMR: Conceptualization, methodology, validation, formal analysis, investigation, writing—original draft, visualization.

AMLA: Conceptualization, validation, writing—review and editing.

MPSP: Resources, writing—review and editing.

ACSCT: Conceptualization, validation, resources, writing (original draft), writing (review and editing), supervision, funding acquisition.

All authors read and approved the final manuscript.

Funding Coordenação de Aperfeiçoamento de Pessoal de Nível Superior – Brasil (CAPES—Coordination for the Improvement of Higher Education Personnel) – Finance Code 001 and grant 88887.340964/2019–00, National Council for Scientific and Technological Development (CNPq) (grant #311230/2020–2) and São Paulo Research Foundation (FAPESP) (grants #2019/24158–9 and 2019/00696–1).

Availability of data and materials All data generated or analyzed during this study are included in this published article and its supplementary information file.

Declarations

Ethics approval and consent to participate Not applicable.

Consent for publication Not applicable.

Competing interests The authors declare that they have no competing interests.

References

ABNT - Associação Brasileira de Normas Técnicas (1992a) ABNT NBR 12619:1992 Versão Corrigida:1995. Waters – determination of nitrite-sulfanilamide and N-(1-naftil) – ethylenediamine methods - Method of test. Rio de Janeiro

ABNT - Associação Brasileira de Normas Técnicas (1992b) ABNT NBR 12620:1992. Waters - determination of nitrate – Chromotropic acid and phenoldissulfonic acid methods - Method of test. Rio de Janeiro

ABNT - Associação Brasileira de Normas Técnicas (1996) ABNT NBR 13736:1996. Water - alkalinity determination potenciometric and titulometric methods - Method of test. Rio de Janeiro

Abreu WWN, Caldeira CRT et al (2020) Automatic vector extraction of water bodies from orbital images, using a language python on the Paranapanema River. Braz J Develop 6:24418–24438. https://doi.org/10.34117/bjdv6n5-045

Acero JL, Stemmler K, von Gunten U (2000) Degradation kinetics of atrazine and its degradation products with ozone and OH radicals: a predictive tool for drinking water treatment. Environ Sci Technol 34:591–597. https://doi.org/10.1021/es990724e

Avetta P, Fabbri D et al (2016) Assessing the phototransformation of diclofenac, clofibric acid and naproxen in surface waters: model predictions and comparison with field data. Water Res 105:383–394. https://doi.org/10.1016/j.watres.2016.08.058

Batista APS, Teixeira ACSC et al (2016) Correlating the chemical and spectroscopic characteristics of natural organic matter with the photodegradation of sulfamerazine. Water Res 93:20–29. https://doi.org/10.1016/j.watres.2015.11.036

Bonmatin JM, Giorio C et al (2015) Environmental fate and exposure; neonicotinoids and fipronil. Enviro Sci Pollut Res 2:35–67. https://doi.org/10.1007/s11356-014-3332-7

Britto FB, Vasco AN et al (2012) Herbicides in the upper Poxim River, Sergipe, and the risk of contamination of water resources. Rev Ciênc Agron 43:390–398. https://doi.org/10.1590/S1806-66902012000200024

Canonica S, Kohn T et al (2005) Photosensitizer method to determine rate constants for the reaction of carbonate radical with organic compounds. Environ Sci Technol 39:9182–9188. https://doi.org/10.1021/es051236b

Carena L, Puscasu CG, Comis S et al (2019) Environmental photodegradation of emerging contaminants: a reexamination of the importance of triplet-sensitised processes, based on the use of 4-carboxybenzophenone as proxy for the chromophoric dissolved organic matter. Chemosphere 237:124476. https://doi.org/10.1016/j.chemosphere.2019.124476

Carena L, Fabbri D et al (2020) The role of direct photolysis in the photodegradation of the herbicide bentazone in natural surface waters. Chemosphere 246:125705. https://doi.org/10.1016/j.chemosphere.2019.125705

Carena L, Comis S, Vione D (2021) Geographical and temporal assessment of the photochemical decontamination potential of river waters from agrochemicals: a first application to the Piedmont region (NW Italy). Chemosphere 263:127921. https://doi.org/10.1016/j.chemosphere.2020.127921

Carlos L, Mártire DO et al (2012) Photochemical fate of a mixture of emerging pollutants in the presence of humic substances. Water Res 46:4732–4740. https://doi.org/10.1016/j.watres.2012.06.022

De Oliveira DM, Cavalcante RP et al (2019) Identification of intermediates, acute toxicity removal, and kinetics investigation to the Ametryn treatment by direct photolysis (UV_{254}), UV_{254}/H_2O_2, Fenton, and photo-Fenton processes. Environ Sci Pollut Res 26:4348–4366. https://doi.org/10.1007/s11356-018-1342-6

Dell'Arciprete ML, Santos-Juanes L et al (2009) Reactivity of hydroxyl radicals with neonicotinoid insecticides: mechanism and changes in toxicity. Photochem Photobiol Sci 7:1016–1023. https://doi.org/10.1039/B900960D

Dell'Arciprete ML, Santos-Juanes L et al (2010) Reactivity of neonicotinoid pesticides with singlet oxygen. Catal Today 151:137–142. https://doi.org/10.1016/j.cattod.2010.01.020

Dell'Arciprete ML, Soler JM et al (2012) Reactivity of neonicotinoid insecticides with carbonate radicals. Water Res 46:3479–3489. https://doi.org/10.1016/j.watres.2012.03.051

Derbalah A, Sunday M et al (2020) Photoformation of reactive oxygen species and their potential to degrade highly toxic carbaryl and methomyl in river water. Chemosphere 244:125464. https://doi.org/10.1016/j.chemosphere.2019.125464

El-Akaad S, Mohamed MA et al (2020) Capacitive sensor based on molecularly imprinted polymers for detection of the insecticide imidacloprid in water. Sci Rep 10:14479. https://doi.org/10.1038/s41598-020-71325-y

Gornik T, Carena L et al (2021) Phototransformation study of the antidepressant paroxetine in surface Waters. Sci Total Environ 774:145380. https://doi.org/10.1016/j.scitotenv.2021.145380

Granado DC, Henry R, Tucci A (2009) Influence of hydrometric level variation on the phytoplanktonic community of the Paranapanema River and a marginal lake in its mouth zone into the Jurumirim Reservoir, São Paulo. Hoehnea 36:113–129. https://doi.org/10.1590/S2236-89062009000100006

Guo J, Shi R et al (2020a) Genotoxic effects of imidacloprid in human lymphoblastoid TK6 cells. Drug Chem Toxicol 43:208–212. https://doi.org/10.1080/01480545.2018.1497048

Guo L, Dai Z et al (2020b) Oligotrophic bacterium *Hymenobacter latericoloratus* CGMCC 16346 degrades the neonicotinoid imidacloprid in surface water. AMB Expr 10:7. https://doi.org/10.1186/s13568-019-0942-y

Helz GR, Zepp RG, Grosby DG (2000) Aquatic and surface photochemistry, 2nd edn. Lewis publisher, Boca Raton

Jacomini AE, de Camargo PB et al (2009) Determination of ametryn in river water, river sediment and bivalve mussels by liquid chromatography-tandem mass spectrometry. J Braz Chem Soc 20:107–116. https://doi.org/10.1590/S0103-50532009000100018

Jacomini AE, de Camargo PB, Avelar WEP, Bonato PS (2011) Assessment of ametryn contamination in river water, river sediment, and mollusk bivalves in São Paulo State, Brazil. Arch Environ Contam

Toxicol 60:452–461. https://doi-org.ez67.periodicos.capes.gov.br/10.1007/s00244-010-9552-z
Kan Q, Lu K et al (2020) Transformation and removal of imidacloprid mediated by silver ferrite nanoparticle facilitated peroxymonosulfate activation in water: Reaction rates, products, and pathways. Environ Pollut 267:115438. https://doi.org/10.1016/j.envpol.2020.115438
Kegley SE, Hill BR, Orme S, Choi AH (2014) PAN Pesticide Database, Pesticide Action Network, North America, CA. http://www.pesticideinfo.org
Kennedy K, Schroeder T et al (2012) Long term monitoring of photosystem II herbicides – correlation with remotely sensed freshwater extent to monitor changes in the quality of water entering the Great Barrier Reef, Australia. Mar Pollut Bull 65:292–305. https://doi.org/10.1016/j.marpolbul.2011.10.029
Kim S, Lee H, Park Y (2017) Perinatal exposure to low-dose imidacloprid causes ADHD-like symptoms: evidences from an invertebrate model study. Food Chem Toxicol 110:402–407. https://doi.org/10.1016/j.fct.2017.10.007
Konstantinou IK, Zarkadis AK, Albanis TA (2001) Photodegradation of selected herbicides in various natural waters and soils under environmental conditions. J Environ Qual 30:121–130. https://doi.org/10.2134/jeq2001.301121x
Kurwadkar S, Evans A et al (2016) Modeling photodegradation kinetics of three systemic neonicotinoids-dinotefuran, imidacloprid, and thiamethoxam-in aqueous and soil environment. Environ Toxicol Chem 35:1718–1726. https://doi.org/10.1002/etc.3335
Lalonde B, Garron C (2020) Temporal and spatial analysis of surface water pesticide occurrences in the maritime region of Canada. Arch Environ Contam Toxicol 79:12–22. https://doi.org/10.1007/s00244-020-00742-x
Lam MW, Tantuco K, Mabury SA (2003) PhotoFate: a new approach in accounting for the contribution of indirect photolysis of pesticides and pharmaceuticals in surface waters. Environ Sci Technol 37:899–907. https://doi.org/10.1021/es025902+
Lastre-Acosta AM, Barberato B et al (2019) Direct and indirect photolysis of the antibiotic enoxacin: kinetics of oxidation by reactive photo-induced species and simulations. Environ Sci Pollut Res 26:4337–4347. https://doi.org/10.1007/s11356-018-2555-4
Lester Y, Sharpless CM, Mamane H, Linden KG (2013) Production of photo-oxidants by dissolved organic matter during UV water treatment. Environ Sci Technol 47:11726–11733. https://doi.org/10.1021/es402879x
Lu Z, Challis JK, Wong CS (2015) Quantum yields for direct photolysis of neonicotinoid insecticides in water: implications for exposure to nontarget aquatic organisms. Environ Sci Technol Lett 2:188–192. https://doi.org/10.1021/acs.estlett.5b00136
Machado CS, Alvez RIS et al (2016) Chemical contamination of water and sediments in the Pardo River, São Paulo, Brazil. Procedia Eng 16:230–237. https://doi.org/10.1016/j.proeng.2016.11.046
Marchetti G, Minella M et al (2013) Photochemical transformation of atrazine and formation of photointermediates under conditions relevant to sunlit surface waters: Laboratory measures and modelling. Water Res 47:6211–6222. https://doi.org/10.1016/j.watres.2013.07.038
Mathon B, Coquery M et al (2019) Influence of water depth and season on the photodegradation of micropollutants in a free-water surface constructed wetland receiving treated wastewater. Chemosphere 235:260–270. https://doi.org/10.1016/j.chemosphere.2019.06.140
McNeill K, Canonica S (2016) Triplet state dissolved organic matter in aquatic photochemistry: reaction mechanisms, substrate scope, and photophysical properties. Environ Sci Process Impacts 18:1381–1399. https://doi.org/10.1039/C6EM00408C
Mitchell C, Brodie J, White I (2005) Sediments, nutrients and pesticide residues in event flow conditions in streams of the Mackay Whitsunday Region, Australia. Mar Pollut Bull 51:23–36. https://doi.org/10.1016/j.marpolbul.2004.10.036
Mnif W, Hassine AIH et al (2011) Effect of endocrine disruptor pesticides: a review. Int J Environ Res Public Health 8:2265–2303. https://doi.org/10.3390/ijerph8062265
Mompelat S, Le Bot B, Thomas O (2009) A model assessment of the occurrence and fate of pharmaceutical products and by-products, from resource to drinking water. Environ Int 35:803–814. https://doi.org/10.1016/j.envint.2008.10.008
Montagner CC, Sodré FF et al (2019) Ten year-snapshot of the occurrence of emerging contaminants in drinking, surface and ground waters and wastewaters from São Paulo state, Brazil. J Braz Chem Soc 30:614–632. https://doi.org/10.21577/0103-5053.20180232
Monteiro RTR, Silva GH et al (2014) Chemical and ecotoxicological assessments of water samples before and after being processed by a Water Treatment Plant. Rev Ambient Água 9:6–18. https://doi.org/10.4136/ambi-agua.1292
Moza PN, Hustert K et al (1998) Photolysis of imidacloprid in aqueous solution. Chemosphere 36:497–502. https://doi.org/10.1016/S0045-6535(97)00359-7
Neto MLF, Sarcinelli PN (2009) Pesticides in drinking water: a risk assessment approach and contribution to the Brazilian legislation updating process. Eng Sanit e Ambient 14:69–78. https://doi.org/10.1590/S1413-41522009000100008
Oliveira NO, Moi GP et al (2014) Congenital defects in the cities with high use of pesticides in the state of Mato Grosso, Brazil. Cien Saude Colet 19:4123–4130. https://doi.org/10.1590/1413-81232014191008512014
Redlich D, Shahin N et al (2007) Kinetical study of the photoinduced degradation of imidacloprid in aquatic media. Clean 35:452–458. https://doi.org/10.1002/clen.200720014
Remucal CT (2014) The role of indirect photochemical degradation in the environmental fate of pesticides: a review. Environ Sci: Process Impacts 16:628–653. https://doi.org/10.1039/C3EM00549F
Rocha AA, Monteiro SH et al (2015) Monitoring of pesticide residues in surface and subsurface water, sediments, and fish in center-pivot irrigation areas. J Braz Chem Soc 26:2269–2278. https://doi.org/10.5935/0103-5053.20150215
Romangnoli I, Manzione RI (2018) Groundwater vulnerability mapping and contamination risks at pontal do Paranapanema region (UGRHI - 22). Braz J Biosyst Eng 12:307–326. https://doi.org/10.18011/bioeng2018v12n3p307-326
Schwarzenbach RP, Gschwend PM, Imboden DM (2003) Environmental organic chemistry, 2nd edn. Wiley & Sons Inc, Hoboken
Shemer H, Sharpless CM et al (2006) Relative rate constants of contaminant candidate list pesticides with hydroxyl radicals. Environ Sci Technol 40:4460–4466. https://doi.org/10.1021/acs.est.7b04439
Silva MP, Mostafa S et al (2015) Photochemical fate of amicarbazone in aqueous media: Laboratory measurement and simulations. Environ Eng Sci 32:730–740. https://doi.org/10.1089/ees.2015.0127
Starling MCVM, Amorim CC, Leão MMD (2019) Occurrence, control and fate of contaminants of emerging concern in environmental compartments in Brazil. J Hazard Mater 372:17–36. https://doi.org/10.1016/j.jhazmat.2018.04.043
Starner K, Goh KS (2012) Detections of the neonicotinoid insecticide imidacloprid in surface waters of three agricultural regions of California, USA, 2010–2011. Bull Environ Contam Toxicol 88:316–321. https://doi.org/10.1007/s00128-011-0515-5
Syafrudin M, Kristanti RA et al (2021) Pesticides in drinking water – a review. Int J Environ Res Public Health 18:468. https://doi.org/10.3390/ijerph18020468
Tarley CRT, Segatelli MG et al (2017) New sorbents based on poly(methacrylic acid-TRIM) and poly(vinylimidazole-TRIM) for simultaneous preconcentration of herbicides in water samples

with posterior determination by HPLC-DAD. RSC Adv 7:37959–37966. https://doi.org/10.1039/C7RA04124A

Todey SA, Fallon AM, Arnold WA (2018) Neonicotinoid insecticide hydrolysis and photolysis: rates and residual toxicity. Environ Toxicol Chem 37:2797–2809. https://doi.org/10.1002/etc.4256

USDA - US Departament of Agriculture (2006) ARS Pesticide Properties. https://www.ars.usda.gov/ARSUserFiles/00000000/DatabaseFiles/PesticidePropertiesDatabase/IndividualPesticideFiles/AMETRYN.TXT

Van Dijk TC, Van Staalduinen AV, Van Der Sluij JP (2013) Macro invertebrate decline in surface water polluted with imidacloprid. PLoS ONE 8:e62374. https://doi.org/10.1371/journal.pone.0062374

Vione DA (2020) A critical view of the application of the APEX software (Aqueous Photochemistry of Environmentally-Occurring Xenobiotics) to predict photoreaction kinetics in surface freshwaters. Molecules 25:9. https://doi.org/10.3390/molecules25010009

Vione D, Scozzaro A (2019) Photochemistry of surface fresh waters in the framework of climate change. Environ Sci Technol 53:7945–7963. https://doi.org/10.1021/acs.est.9b00968

Vione D, Das R et al (2010) Modelling the occurrence and reactivity of hydroxyl radicals in surface waters: implications for the fate of selected pesticides. Int J Environ Anal 90:260–275

Vione D, Maddigapu PR et al (2011) Modelling the photochemical fate of ibuprofen in surface waters. Water Res 45:6725–6736. https://doi.org/10.1016/j.watres.2011.10.014

Vione D, Encinas A et al (2018) A model assessment of the potential of river water to induce the photochemical attenuation of pharmaceuticals downstream of a wastewater treatment plant (Guadiana River, Badajoz, Spain). Chemosphere 198:473–481. https://doi.org/10.1016/j.chemosphere.2018.01.156

Wang Y, Fan L et al (2020) Photodegradation of emerging contaminants in a sunlit wastewater lagoon, seasonal measurements, environmental impacts and modelling. Environ Sci: Water Res 6:3380–3390. https://doi.org/10.1039/D0EW00527D

Wu B, Arnold WA, Ma L (2021) Photolysis of atrazine: role of triplet dissolved organic matter and limitations of sensitizers and quenchers. Water Res 190:116659. https://doi.org/10.1016/j.watres.2020.116659

Zaror C, Segura C et al (2010) Kinetic study of imidacloprid removal by advanced oxidation based on photo-Fenton process. Environ Technol 31:1411–1416. https://doi.org/10.1080/09593331003680926

Zeng T, Arnold WA (2013) Pesticide photolysis in prairie potholes: probing photosensitized processes. Environ Sci Technol 47:6735–6745. https://doi.org/10.1021/es3030808

Zhang P, Shao Y et al (2020) Phototransformation of biochar-derived dissolved organic matter and the effects on photodegradation of imidacloprid in aqueous solution under ultraviolet light. Sci Total Environ 724:137913. https://doi.org/10.1016/j.scitotenv.2020.137913